

3d transition-metal impurities in aluminum

Diola Bagayoko and Pui-Man Lam

Department of Physics, Southern University and A&M College, Baton Rouge, Louisiana 70813-1776

Nathan Brener

Department of Computer Science, Louisiana State University and A&M College, Baton Rouge, Louisiana 70803-4001

Joseph Callaway*

Department of Physics and Astronomy, Louisiana State University and A&M College, Baton Rouge, Louisiana 70803-4001

(Received 5 January 1996; revised manuscript received 14 May 1996)

We report the electronic and magnetic structures and the density of states of 3d transition-metal impurities, from vanadium to nickel, in a fcc aluminum matrix. The free clusters Al_{19} and $Al_{18}M$, where M stands for V, Cr, Fe, Co, and Ni, have been studied at a lattice constant of 7.635 a.u. Our *ab initio*, all-electron, and self-consistent calculations utilized a local density potential and symmetrized Gaussian basis functions. A net and substantial spin polarization of the Al atoms surrounding the impurity is found in all cases except for Cr. Local moments greater than $1\mu_B$ exist on Cr and Mn impurities. While the cluster moment is zero for $Al_{18}Fe$, local moments of $0.008\mu_B$ and $0.14\mu_B$ are found on the iron impurity, indicating multiple spin states. We reproduce the experimentally found maximum d influence at the Fermi level for chromium. [S0163-1829(96)03141-4]

INTRODUCTION

The current interest¹⁻¹¹ in aluminum alloys is partly sustained by recent advances in experimental and theoretical investigations. In particular, properties of AlM alloys, where M stands for a 3d transition metal, are being revisited, experimentally as well as theoretically, following the discovery of the icosahedral structure⁷ of $AlMn$. It has recently been established⁸ that AlM , $M=V, Cr, Mn, Fe, Co,$ and Ni , can exist in an icosahedral phase, particularly at impurity concentrations above 10 at. %. The work of Hauser *et al.* on $AlMn$ considered the face-centered-cubic (fcc) and icosahedral structures. Hauser *et al.*¹⁰ found a local moment of $1.55\mu_B$ on Mn in fcc aluminum films for a concentration of 5 at. %. Our previous theoretical result¹¹ of a local moment of $1.74\mu_B$ on Mn, in the $Al_{18}Mn$ free cluster, reasonably agrees with the above finding for fcc alloys of concentration of 5 at. %. Like Bagayoko *et al.*, de Coulon, Reuse, and Khanna² employed the linear combination of Gaussian orbitals (LCGO's) and a local density functional potential in *ab initio*, self-consistent calculations of properties of Al_nMn free clusters. They considered icosahedral and cubic geometries. They recently reported local moments of about $4.0\mu_B$, $2.05\mu_B$, and $1.65\mu_B$ on Mn in the $Al_{12}Mn$, $Al_{18}Mn$, and $Al_{26}Mn$ free clusters in cubic geometry, respectively. Their result for $Al_{18}Mn$, around $2.05\mu_B$, is comparable to that of Bagayoko *et al.*¹¹

Several authors¹²⁻¹⁵ discussed theoretically models of dilute magnetic alloys. Actual self-consistent calculations of the electronic structure or density of states of fcc AlM alloys are relatively recent^{11,16-18} and limited. Scattering calculations based on Anderson's theory and employing model potentials¹⁶⁻²² mainly provided the relevant parameters including the width of the virtual bound states and their separations from the Fermi level. The jellium model calculations

of Nieminen and Puska¹⁶ led to a local moment of $2.46\mu_B$ on Mn impurity in aluminum.

Deutz, Dederichs, and Zeller¹⁷ studied several 3d impurities in aluminum, using a von Barth-Hedin-type local density potential. Their Korringa-Kohn-Rostoker- (KKR-) Green function calculations assumed the host aluminum potential to remain unchanged from that of the elemental Al metal. They computed self-consistently the potential at the site of the impurity in an otherwise unperturbed infinite aluminum metal. These authors found $AlCr$, $AlMn$, and $AlFe$ to be magnetic, with local moments of $2.0\mu_B$, $2.5\mu_B$, and $1.75\mu_B$, respectively, located on Cr, Mn, and Fe. They reported no local moments in the cases of vanadium, cobalt, and nickel impurities. Singh⁶ performed computations of the electronic structure of 489-atom clusters of fcc aluminum with a substitutional 3d transition-metal impurity at the center. As in the work of Deutz *et al.*, the host aluminum potential was assumed to be unchanged in these relatively recent calculations. Singh employed the recursion method and a tight-binding linear muffin-tin orbital Hamiltonian and reported agreements with the results of Deutz *et al.* Kurkina *et al.*¹ recently reported qualitative agreements with the results of Deutz *et al.* for Al_nFe , Al_nCo , and Al_nNi , with the subscript n varying from 5 to 88. These authors employed local density functional potentials in their "atom embedded in a jellium sphere" calculations. Postnikov *et al.*¹⁸ obtained a nonmagnetic ground state for $Al_{12}Fe$ embedded clusters. Their scattering wave calculations employed an X_α potential. Both the impurity and host potentials were treated self-consistently by these authors. Guenzburger and Ellis³ conducted first-principle, density functional calculations of properties of $Al_{18}Fe$ and $Al_{42}Fe$ embedded clusters. They found local moments on iron of $0.44\mu_B$ and $0.96\mu_B$ for $Al_{18}Fe$ and $Al_{42}Fe$, respectively. The respective cluster moments were $0.09\mu_B$ and $0.55\mu_B$. An important finding of these authors

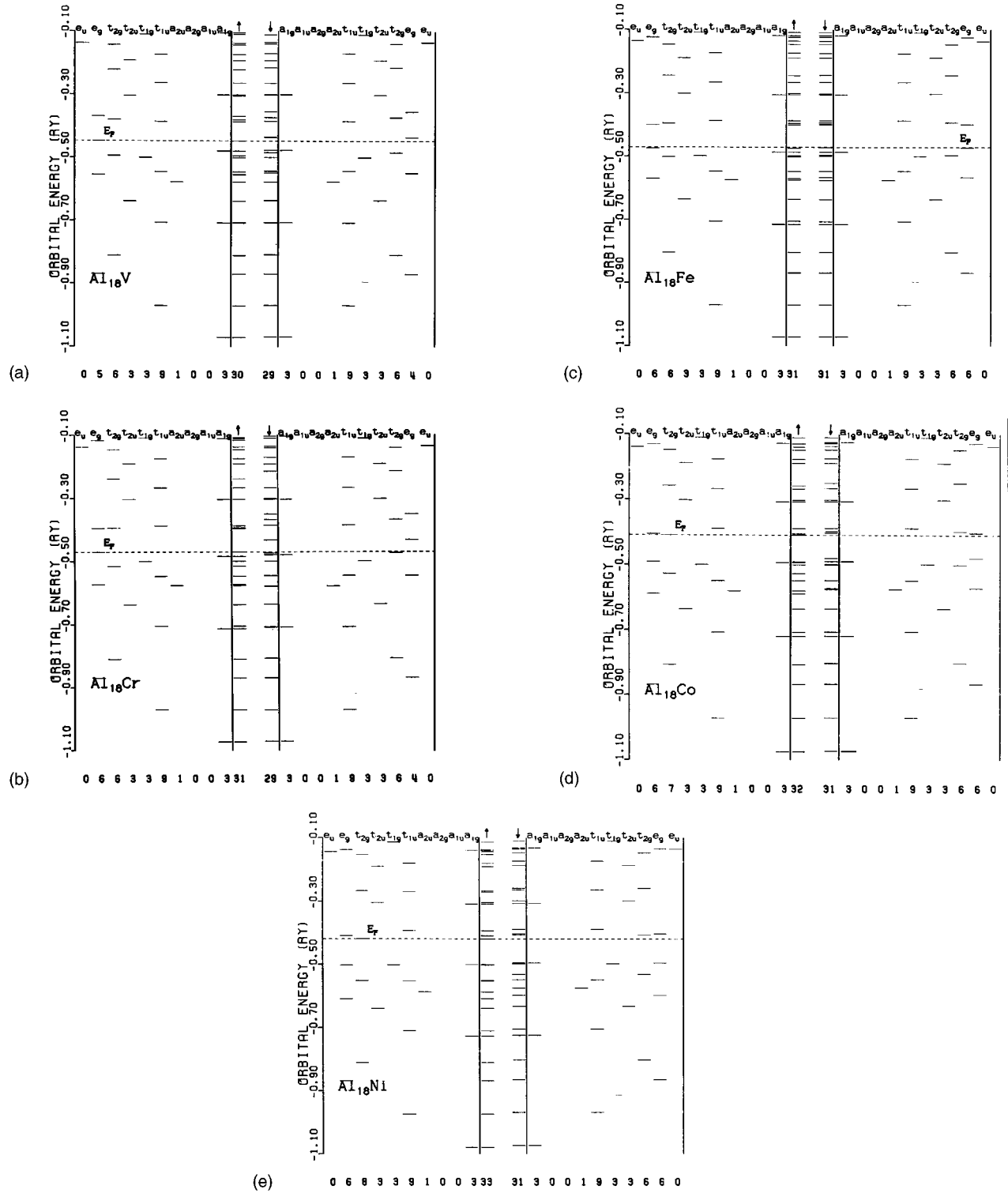


FIG. 1. Energy level diagrams for $\text{Al}_{18}M$ clusters. Up and down spin levels are, respectively, shown on the left and right portions of each diagram. The numbers at the bottom of a diagram are the total occupancies of states whose symmetry is specified at the top of the diagram. (a) Al_{18}V , (b) Al_{18}Cr , (c) Al_{18}Fe , (d) Al_{18}Co , and (e) Al_{18}Ni .

consists of the vanishing of the local and cluster moments, for Al_{42}Fe , when the relaxation of the nearest-neighbor aluminum atoms is taken into account.

Until recently, 3d transition-metal impurities in aluminum were believed to have nonmagnetic ground states described by the Anderson model.¹² The above survey of previous theoretical works clearly raises questions about the

magnetic state of $\text{Al}M$ systems. The aim of this paper is to investigate the electronic and magnetic properties of $\text{Al}_{18}M$ clusters. The free clusters we consider have increasing technological and scientific importance, due in part to the current capability of preparing them in varying sizes and geometries.⁹ Additionally, the electronic and magnetic properties of clusters are needed for understanding the transition

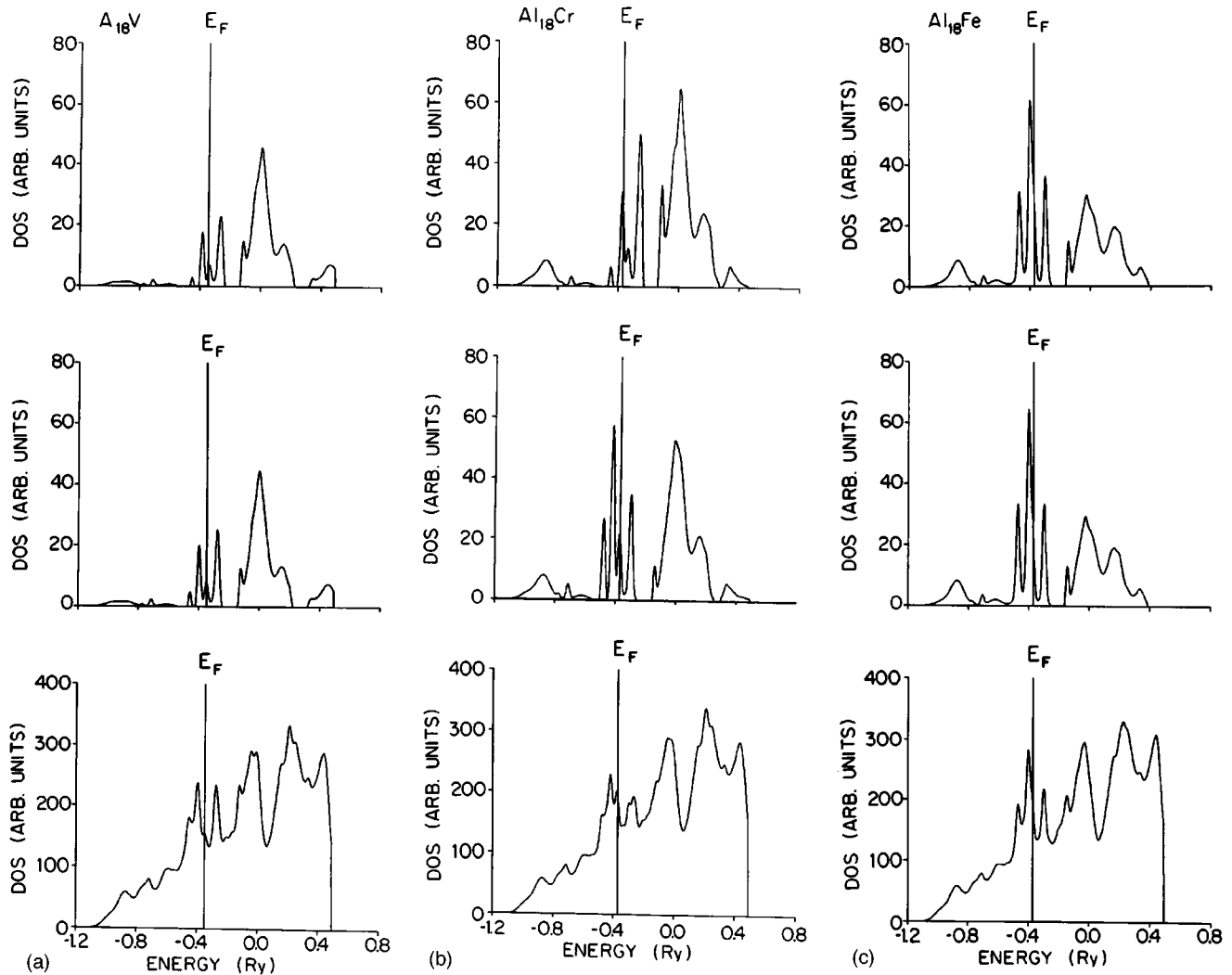


FIG. 2. Cluster density of states for $\text{Al}_{18}M$. (top) Impurity partial d density of states for minority spin, (middle) impurity partial d density of states for majority spin, and (bottom) total density of states for the cluster: (a) Al_{18}V , (b) Al_{18}Cr , (c) Al_{18}Fe , (d) Al_{18}Co , and (e) Al_{18}Ni .

from atoms to infinite systems. Our motivations are further reinforced by the good agreement between our previous results, for Al_{18}Mn , and the findings of the meticulous experimental work of Hauser *et al.*¹⁰

The corroboration of our results, for manganese, by first-principles calculations, very similar to ours, of de Coulon *et al.*² is an added indication of the contribution intended with our present work. Finally, this work presents *ab initio*, self-consistent calculations of the electronic structures and related properties of $\text{Al}_{18}M$, without frozen core or unperturbed host approximations, that span the $3d$ series from vanadium to nickel.

METHOD

The species studied are free clusters of 19 atoms in a fcc geometry. The central atom is, respectively, surrounded by the 12 and 6 nearest- and next-nearest-neighbor aluminum atoms. Except in the case of Al_{19} , this central atom is a $3d$ transition element. The fcc lattice constant of 7.635 a.u. is chosen to be that of metallic aluminum.

Details of our computational method are available from previous works of this group.^{11,23,24,27} The Rajagopal-

Singhal-Kimball²⁵ (RSK) local density potential was employed in a linear combination of Gaussian orbital (LGO) formalism. Uncontracted, i.e., independent, Gaussians were used in the generation of symmetrized basis functions.^{26,27} Our all-electron calculations entailed no frozen core approximation. Impurity and host atom potentials are treated self-consistently. Matrix elements of the exchange correlation potential are evaluated numerically. A supplementary charge fitting of the type described by Mintmire and Dunlap²⁸ is employed in the calculation of the matrix elements of the Coulomb potential.^{26,27}

To guarantee further the proper description of the charge redistribution in the cluster environment, as opposed to that of an isolated atom, diffuse s and p orbitals were added to the atomic basis set for aluminum. Polarization was provided for with the inclusion of d orbitals in the aluminum basis set. The aluminum basis set is as reported in Ref. 11, at the exclusion of the smallest d exponent of 0.21. The aluminum basis consisted of $12s$, $9p$, and $4d$. The basis sets for the transition elements were those reported²⁹ by Watchers, including the diffuse p orbitals for the excited states. These basis sets comprised $14s$, $11p$, and $5d$ Gaussian orbitals. We

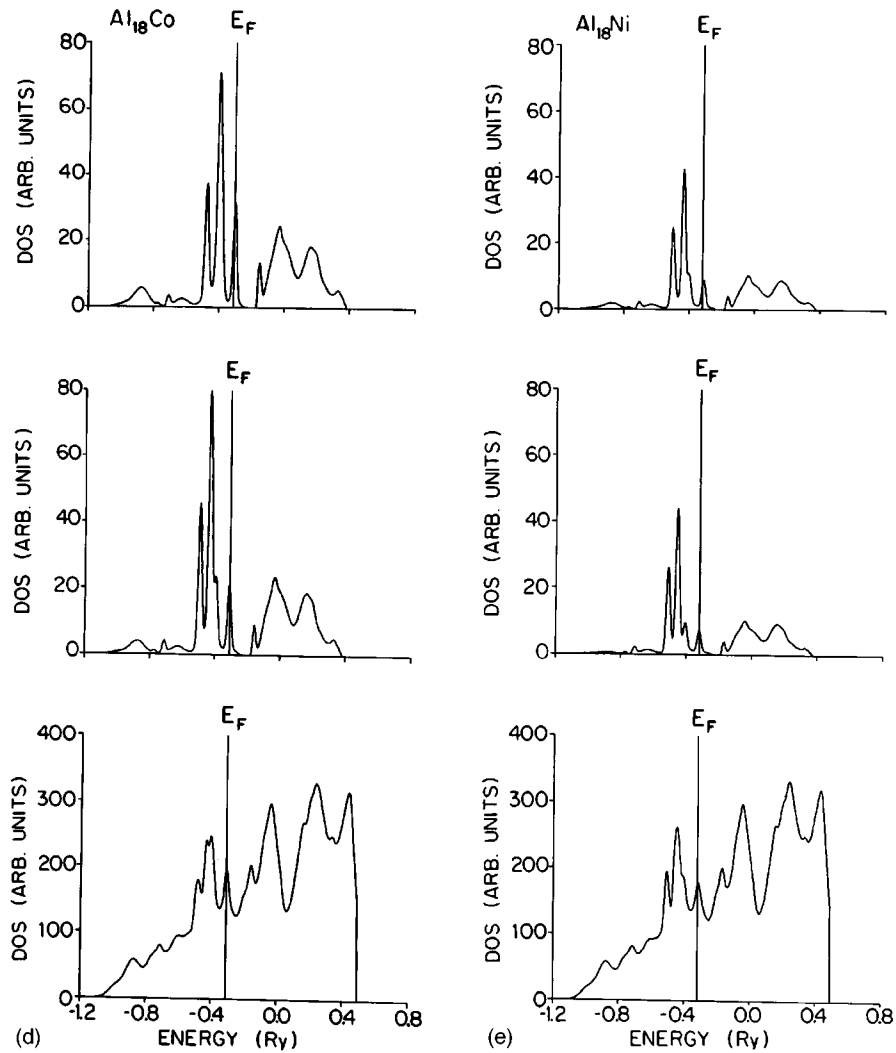


FIG. 2. (Continued).

previously reported¹¹ the results for Al_{18}Mn obtained with larger basis sets on the impurity and the aluminum atoms. The basis sets for the present calculations were the largest ones, for $\text{Al}_{18}M$, where M stands for V, Cr, Fe, Co, and Ni for which no numerical difficulties arose. These difficulties included negative values in the Mulliken population analysis results for occupied states. The reduction of the sizes of the basis sets consisted of dropping the even-tempered d exponents for M and the smallest d exponent for Al. Numerous computational tests were run in the process. The resulting basis sets, described above, were the largest ones for which no numerical difficulties were encountered.

In light of the above case for Mn, answering the question of the stability of our results with respect to the selected basis sets (for Al and M) led to numerous tests over several years. While we could make educated speculations as to the possible answer, based in part on Hund's rule, the number of d electrons, and the coordination number, the complexity of the actual cluster environment demanded that we perform these tests where the even-tempered exponents were dropped one at a time. The Watchers basis sets, for transition elements other than Mn, were found to be the largest possible. We conducted a few tests in which the basis sets were reduced from their largest sizes. Even the reduction of these

basis sets by two p orbitals on M and by two d orbitals on Al did not make a significant difference. For Mn, for instance, this led to a self-consistent local moment of $1.998\mu_B$. This value is basically equal to the $2.06\mu_B$ obtained with 11 p orbitals on Mn and 4 d orbitals on Al. Dropping the two p orbitals with the smallest exponents on Al, however, led to clearly wrong answers for the energies and the magnetic moment. This last result was predictable, given the sp character of aluminum. The overall outcome of these tests was that the results reported here are very stable with respect to reasonable changes in the basis sets.

Our calculations did not entail changes of the input electronic configuration in the sense of Hartree-Fock calculations. The changes made from the ground state configurations of the free atoms of Al or M consisted of redistributing the electrons, in the uppermost s , p , or d valence states, between the up and down spin. These changes were made to vary the input magnetic moment as noted above. Density functional calculations, as compared to those of the Hartree-Fock type, have inherent limitations with respect to changing input configurations.

With the above formalism, completely self-consistent and spin-polarized calculations were carried out for Al_{19} and $\text{Al}_{18}M$, where M stands for V, Cr, Fe, Co, and Ni. Self-

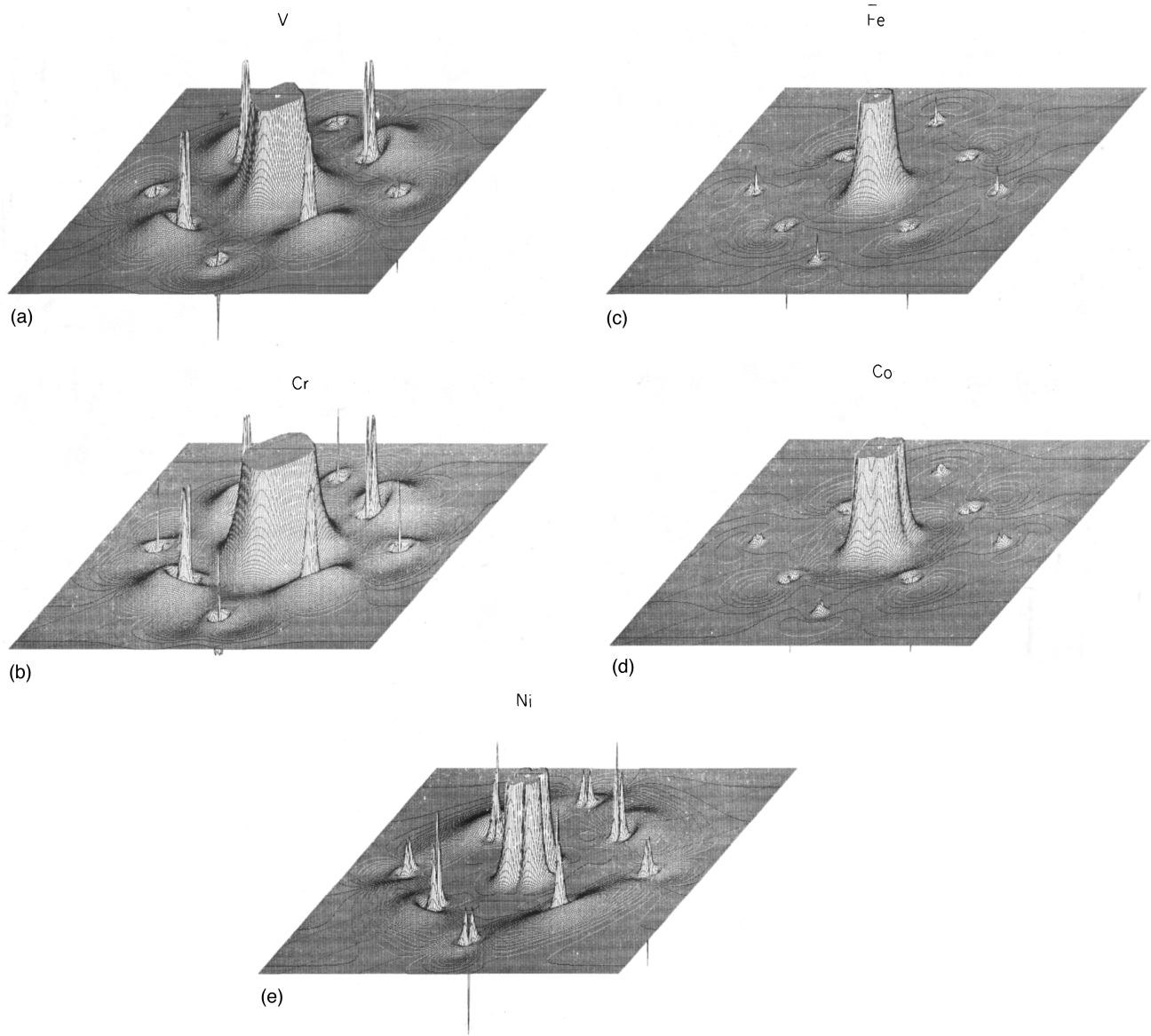


FIG. 3. Spin-density distribution of Al_{18}M in the (100) plane. The range of plotted values is from -0.01 to $+0.01$; the heights of the major peaks around the nuclei are truncated; the fine structures in interatomic regions are fully exhibited: (a) Al_{18}V , (b) Al_{18}Cr , (c) Al_{18}Fe , (d) Al_{18}Co , and (e) Al_{18}Ni .

consistency was reached, in all cases, within 465 iterations. We conducted a test of a possible variational stiffness stemming from relatively large input magnetic moments. It was feared that small local moments on the impurity may be due to a relatively slow convergence of the magnetic moment even though other parameters, i.e., electronic energies, may be converged. The results reported here for V, Co, and Ni were obtained twice. The first calculations utilized input moments of $3\mu_B$, $3\mu_B$, and $2\mu_B$ for V, Co, and Ni, respectively. The input moments for the second calculations were $0.5\mu_B$, $0.4\mu_B$, and $0.2\mu_B$ for V, Co, and Ni, respectively. These second input moments were at most 0.1 smaller (for V) or 0.2 larger (for Ni) than the magnetic moments that resulted from the first calculations. The only difference observed between the two calculations, for each impurity, consisted of a very rapid convergence in the case of small input moments, in less than 180 iterations, as compared to the first calculations that generally took 360–460 iterations. The case

of iron is noted in the section devoted to the discussion. We report below the electronic energy levels, magnetic properties, and density of states of Al_{18}M clusters.

RESULTS

The electronic energy levels are provided in Figs. 1(a)–1(e). Figures 2(a)–2(e) describe the density of d states for the central atoms as well as the total cluster density of states. Figures 2(a) (top), 2(b) (middle), and 2(c) (bottom) are, respectively, for the minority spin d density of states, majority spin d density of states, and the total density of states for the Al_{18}V cluster, as an example. Figures 3(a)–3(e) show the spin density distributions. The Mulliken population analysis results are in Table I. Table II shows the states at the Fermi level, the occupancy of these states, the local magnetic moments on the impurities, and the total cluster moments. We

TABLE I. Mulliken population analysis, from the integrated cluster density of states (CDOS), for Al_{19} and $\text{Al}_{18}M$, $M = \text{V, Cr, Mn, Fe, Co, and Ni}$. Results for Al_{18}Mn are from the second calculations with Watchers (Ref. 29) basis set (smaller than that used in Ref. 11).

	Al_{18}Al	Al_{18}V	Al_{18}Cr	Al_{18}Mn	Al_{18}Fe	Al_{18}Co	Al_{18}Ni
Central atom							
$sp\uparrow$	2.396	0.152	1.064	1.703	1.841	1.578	1.379
$sp\downarrow$	2.421	0.068	1.067	1.884	1.854	1.786	1.686
$d\uparrow$	0.031	1.944	3.196	3.798	3.290	4.012	4.360
$d\downarrow$	0.027	1.457	1.188	1.557	3.136	3.413	4.040
Total	4.875	3.621	6.515	8.942	10.121	10.789	11.465
First shell							
$sp\uparrow$	1.425	1.539	1.457	1.353	1.379	1.420	1.482
$sp\downarrow$	1.359	1.487	1.427	1.432	1.392	1.372	1.330
$d\uparrow$	0.016	0.015	0.015	0.014	0.014	0.015	0.016
$d\downarrow$	0.014	0.016	0.016	0.015	0.014	0.014	0.013
Total	2.814	3.057	2.915	2.814	2.799	2.821	2.841
Second shell							
$sp\uparrow$	1.537	1.531	1.504	1.506	1.515	1.523	1.538
$sp\downarrow$	1.501	1.566	1.563	1.523	1.514	1.520	1.517
$d\uparrow$	0.008	0.009	0.009	0.009	0.009	0.009	0.009
$d\downarrow$	0.008	0.009	0.008	0.009	0.009	0.009	0.008
Total	3.054	3.115	3.085	3.047	3.047	3.061	3.072

provide the spin densities at the sites of the nuclei in Table III.

A simple pattern characterizes the states at the Fermi level. For Al_{19} , the total occupancy of the $\Gamma_{25'}\downarrow$ at the Fermi level is two (2) electrons. Up and down arrows, respectively, stand for majority (up) and minority (down) spin states. The states at the Fermi level are $\Gamma_{12}\uparrow$, $\Gamma_{12}\uparrow$, $\Gamma_{12}\downarrow$, $\Gamma_{12}\downarrow$, $\Gamma_{25'}\uparrow$, and $\Gamma_{25'}\uparrow$, respectively, for V, Cr, Mn, Fe, Co, and Ni impurities with respective occupancies of 1, 2, 1, 2, 1, and 2. The behavior of the energy levels across the 3d series is best apparent in Figs. 2(a)–2(e). The Anderson-type virtual bound states can be found at the Fermi level for chromium, as shown in Fig. 2(a) (top). The graph of the density of state for Al_{18}Mn , in Ref. 11, indicates that the peaks in the d density of states are already below E_F for this system. This clearly reproduces the experimentally found maximum d influence³⁰ at the Fermi level for Cr. A measure of this d

TABLE II. Symmetry of the state at the Fermi level (E_F), the occupancy at the Fermi level, the local moment on the central atom, in Bohr magnetons (μ_B), and the cluster moment (in μ_B) for Al_{19} and $\text{Al}_{18}M$, $M = \text{V, Cr, Mn, Fe, Co, and Ni}$. The local moments reported here include the sp and d contributions which are separately available from Table I. The calculated local moment for Mn, using (Ref. 11) larger and more complete basis sets, is $1.74\mu_B$.

Cluster	State at E_F	Occupancy at E_F	Local moment	Cluster moment
Al_{18}Al	$\Gamma_{25'}\uparrow(t_{2g})$	2	-0.021	1
Al_{18}V	$\Gamma_{12}\uparrow(e_g)$	1	+0.571	1
Al_{18}Cr	$\Gamma_{12}\uparrow(e_g)$	2	+2.005	2
Al_{18}Mn	$\Gamma_{12}\downarrow(e_g)$	1	+2.060	1
Al_{18}Fe	$\Gamma_{12}\downarrow(e_g)$	2	+0.142	0
Al_{18}Co	$\Gamma_{25'}\uparrow(t_{2g})$	1	+0.391	1
Al_{18}Ni	$\Gamma_{25'}\uparrow(t_{2g})$	2	+0.013	2

influence is the zero-temperature value of the impurity resistivity; this value is the largest for Cr, followed by Mn, as compared to the other impurities.³⁰ The parabolic dependence of the low-field Hall coefficient on the impurity, with the minimum at Cr, is interpreted³⁰ in terms of the location of the virtual bound states with respect to the Fermi level. As one moves from Cr to Ni, these states progressively sink below the Fermi energy and their densities get narrower, as expected.

The Mulliken population analysis of the integrated density of states, shown in Table I, reveals a gain of electrons by the central impurity, except in the case of vanadium. While Mulliken population data are not highly accurate in general, we consider our accounting for all electrons in the system to be an added indication of the quality of our wave functions. Specifically, the total numbers of valence electrons as shown in Table I, for the respective systems, do not deviate by more than 0.06 from their exact values. This maximum deviation is actually of the order of 10^{-3} when the results in Table I are listed up to the fourth decimal place.

Table II provides the local and cluster moments for the systems considered. A local moment of $2.005\mu_B$ is found on the chromium impurity. A moment around $2.0\mu_B$ is located on manganese, as discussed below. The local moments on the other impurities are around or smaller than $0.5\mu_B$. The local moment on iron is $0.14\mu_B$, while the cluster moment is zero, for calculations where the initial input moment is $4\mu_B$. These small moments (i.e., less than 1) were the reason we performed the calculations twice, as noted above. A net (sum of positive and negative ones) spin polarization of the surrounding aluminum atoms is found in all cases, except for the chromium impurity. The local and cluster moments are practically equal for chromium, while they are quite different for the other 3d elements. The total or net polarization of surrounding aluminum atoms constitutes a compensation cloud for manganese and iron impurities, while for vanadium, cobalt, and nickel it adds to the local moment to yield

TABLE III. Spin density at the nuclei (in $e/a.u.^3$) for Al_{19} and $Al_{18}M$, $M=V, Cr, Mn, Fe, Co,$ and Ni . The data for $Al_{18}Mn$ are from Ref. 11.

	Al_{19}	$Al_{18}V$	$Al_{18}Cr$	$Al_{18}Mn$	$Al_{18}Fe$	$Al_{18}Co$	$Al_{18}Ni$
Central atom	-0.011	-0.041	-0.122	-0.108	-0.008	-0.061	-0.071
	Al_{12} +0.012	+0.111	+0.173	+0.030	-0.009	-0.008	+0.025
	Al_6 -0.007	-0.009	+0.007	+0.028	+0.003	-0.0004	-0.013

a cluster moment larger than that on the impurity. This pattern is particularly pronounced for nickel where both the first- and second-shell aluminum atoms are surrounded with ferromagnetic (i.e., positive—in the same direction as that on the impurity) polarization. In the case of chromium, the net polarization of host aluminum atoms is negligible; the rather large and positive polarization around the nearest-neighbor aluminum atoms is compensated by the large negative polarization and smaller negative polarization, respectively, around the second- and first-shell aluminum atoms. This explains the fact that the local and cluster moments are the same for $Al_{18}Cr$. The small local moment of $0.013\mu_B$, for $Al_{18}Ni$, results from a compensation of the contribution of 0.320 from the nickel d electrons by an sp contribution also located on the impurity. The cluster moment of $2\mu_B$ is mostly due to contributions from the first-shell aluminum atoms. The qualitative behavior of the polarization around the host aluminum atoms, as described above, is partly apparent from Figs. 3(a)–3(e) that show the spin-density distribution in the (100) plane.

We paid a particular attention to $Al_{18}Fe$, due to known rapid variations of the spin moment of iron in the fcc geometry, as noted in the discussion section below. While more work is ongoing for this system, we already have a picture of the variation of the local moment on the iron impurity with the lattice constant. For lattice constants of 7.935, 7.635, 7.560, and 7.485 a.u., the self-consistent local moments on Fe, for an input moment of $4.0\mu_B$, are, respectively, $0.365\mu_B$, $0.138\mu_B$, $0.110\mu_B$, and $0.085\mu_B$. The respective total energies per atom are -589.229 , -589.795 , -589.801 , and -589.775 Ry. These total energy results predict the existence of this free cluster in nature at a lattice constant of 7.560 a.u. where the minimum total energy is found.

A question arose as to the electronic and magnetic properties of $Al_{18}Mn$ if they are calculated using the Watchers' wave functions²⁹ as done for the other elements in the $3d$ series. We answered it by recalculating the properties of this system using Watchers' basis set, including the excited p orbitals, and the aluminum basis set described above. The state and occupancy at the Fermi level were found to remain unchanged. The energy levels were rigidly shifted upward in absolute value. This shift is an intrinsic property of the Ritz variational method; the true eigenvalues are asymptotically approached as the basis set gets larger, provided that linear dependence or other numerical difficulties do not arise. The discernible changes from the results of Bagayoko *et al.*¹¹ were a gain of 0.73 electron by the impurity and a new local moment of $2.06\mu_B$. The deletion of the Gaussian functions with small even-tempered d exponents from the basis set for Mn explains the loss by the d states and gain by the sp states of 2 of the Mn valence electrons, as compared to the results of Bagayoko *et al.* The increase of 0.32 in the moment on

Mn, as compared to the previous result of $1.74\mu_B$, is the sum of variations in the Mulliken population. Physically, this increase is to be expected as a decrease in the basis set, particularly with the absence of very dilute exponents, favors moment forming intra-atomic interaction at the expense of interatomic hybridization which destroys the magnetic moment. While the local moment of $2.06\mu_B$ is meaningful, our preferred local moment for $Al_{18}Mn$ is $1.74\mu_B$, as the latter resulted from calculations that employed more complete basis sets. The calculations reported here for the other $3d$ elements, as noted in the section on our method, were first done with the extended basis sets similar to those in Ref. 11. Numerical difficulties led to the reduced basis sets as explained above.

The largest exchange splittings, for valence states below or across the Fermi level, are, respectively, 0.162, 0.579, 0.06, 0.366, and 0.269 eV for $Al_{18}M$, $M=V, Cr, Fe, Co,$ and Ni . These values occur at the $\Gamma_{25'}$ or t_{2g} state, except for vanadium where it is at Γ_{12} . Some values of the exchange splittings for $Al_{18}Mn$, as previous discussed by Bagayoko *et al.*,¹¹ are between 0.5 and 0.7 eV. There are no optical transition data, as in the case of copper alloys, to permit a meaningful comparison.

Figures 2(a)–2(e) display the cluster density of states. Different scales are employed for the d density of states. The heights of the impurity d density of states at E_F are 21.92, 51.22, 28.78, 23.82, and 22.34 states per Rydberg respectively for V, Cr, Fe, Co, and Ni impurities. The d influence at the Fermi level is maximum for $Al_{18}Cr$ in both relative and absolute terms. The d density of states at E_F , for Cr, is much larger than those for the other impurities and it is almost as large as the highest d peak for occupied states, which is 59.63 for $Al_{18}Cr$. For the other impurities, the value of the d density of states at E_F is a factor of 2–4 times smaller than the highest d peak for occupied states.

DISCUSSION

Some basic points relevant to a comparison of our findings with experiment and other calculations include the lattice structure and parameter we considered, the exclusion of temperature effects in our zero-temperature calculations, the impurity concentration, and long-range interactions which are not accounted for in free and finite cluster calculations. Despite these possible sources of differences between our results and measurements on dilute alloys, we have reproduced some basic features which are experimentally established.

The sinking below the Fermi level and the associated narrowing of the d density of states, as the atomic number of the impurity increases, are particularly apparent from our results. The experimentally known maximum d influence at the

Fermi level for chromium is unambiguously reproduced.³⁰

The extensive experimental data on AlM alloys, as reviewed by Rizzuto,³⁰ mostly pertained to concentrations much smaller than 5 at. % appropriate for Al₁₈M clusters. Cooper and Miljak³¹ reported static susceptibility results for AlV, AlCr, and AlMn alloys among others. They reported a Curie-Weiss behavior of the spin susceptibility for AlMn following an elaborate analysis. This analysis took into account the strong thermal effect on the susceptibility, believed to be mostly due to the host aluminum. These authors basically assumed that variations in the susceptibility of AlV and AlCr, which could have been interpreted in terms of a Curie-Weiss behavior, to be due to the above spurious thermal effect and an alloying effect distinct from the intrinsic contribution of the impurity. Taking the parallel results (curves) for AlV and AlCr as base lines, they obtained the magnetic results for AlMn. This magnetism was presumed to be masked by the above spurious effects. They recognized that other interpretations of the data were possible. These authors considered quenched samples with dislocations and for concentrations below 2 at. %. This work illustrates experimental difficulties, some of which have been elucidated by Wohllben and Coles.¹⁴ One could speculate that had the assumption of nonmagnetic state for V and Cr in aluminum not been made by these authors, based mainly on the expected nonmagnetic behavior for V, their work could have provided a picture consistent with theoretical findings relative to the presence of local moments on vanadium, chromium, and manganese impurities in aluminum. The impurity electrical resistance measurements by Caplin and Rizzuto,³² for dilute AlCr and AlMn (*M* concentrations of 0.2–0.04 at. %), were explained using the localized spin fluctuation model, appropriate for an intermediate state between the magnetic and nonmagnetic states as described by the Friedel-Anderson model. The dependence of the impurity resistance on temperature, one of the experimental signature of magnetism, was obtained. The x-ray photoemission spectroscopy results of Steiner *et al.*³³ suggested the existence of a local moment on Mn in aluminum, at least on a short time scale. They inferred the presence of a local moment from their finding of a significant *3s* splitting. It should be noted, however, that van Acker *et al.*³³ recently found the *3s* splitting, in the case of iron impurities, not to be a reliable predictor of the existence of a local moment.

The experimental picture of the magnetic state of 3d impurities in aluminum, first believed to be mostly nonmagnetic, is questioned by recent findings. The extensive experimental studies by Dunlap and co-workers³⁴ reported small average moments per Fe atom for Al₈₆Fe₁₄ alloys. Their crystalline and rapidly quenched samples exhibited room-temperature average moments, per Fe atom, of 0.002μ_B and 0.026μ_B respectively. Our calculated local moment of 0.14μ_B for iron, for an input moment of 4μ_B, is much larger than their estimate and much smaller than the 0.44μ_B reported by Guenzburger and Ellis³ for Al₁₈Fe. There are plausible reasons for the difference between these calculated results and the above experimental estimates. They include the difference in Fe concentration and that of the systems. Also, our results are expected to differ from those of Guenzburger and Ellis on account of the difference in the systems. They considered embedded clusters, while we treated isolated

ones. From basic moment formation mechanism,^{12–15} however, the local moment on Fe in the isolated cluster is expected to be higher than that on the embedded one.

The above picture of the magnetic state of iron impurities in aluminum is further complicated by the results of computational experiments we conducted. Like in the cases of V, Co, and Ni, we performed several self-consistent calculations of the properties of Al₁₈Fe with different input magnetic moments. The self-consistent final moments on the iron impurity changed with the input moment, indicating possible multiple spin states for this cluster. Details of these experiments are to be reported in a manuscript under preparation. The salient point consists of the finding of local moments of 0.0077μ_B and 0.1379μ_B for input moments of 0.2μ_B and 4.0μ_B, respectively, at the same lattice constant of 7.635 a.u. Possibilities of computational artifacts are unlikely due to the fact that similar computations for V, Co, and Ni, with input moments slightly below or above the results of the first calculations, rapidly converged to the first results obtained with much larger input moments. While this is the first indication we know of different magnetic moment states for this finite cluster, a similar behavior was reported for clusters of 3d elements³⁷ and for metallic iron in fcc geometry.^{38–41}

The subtlety of the issue of magnetism, for transition-metal impurities in aluminum, is somewhat underscored by the absence of a moment in fcc AlMn at concentrations below 2% as discussed by Hauser *et al.*¹⁰ These authors also found a local moment on Mn impurities in icosahedral aluminum. The local moment on Mn, in fcc AlMn films, was measured to be 1.55μ_B for Mn concentrations around 5 at. %. These authors reported local moments on Mn in amorphous and crystalline AlMn for a variety of concentrations up to 45 at. %. We are unaware of recent and refined measurements similar to those of Hauser *et al.* for other *M* alloys at concentrations around 5 at. %. The calculated local moment¹¹ of 1.74μ_B on Mn, as previously discussed, agrees with the recent measurements.¹⁰ The intra-atomic interactions that are responsible for moment formation lead to larger moments in a free clusters as compared to a thin film, as long as concentrations are not so high that an impurity-impurity influence creates added difficulties. In this sense, even our reduced-basis computational result of 2.06μ_B, which is about the same as the 2.05μ_B Mn local moment of de Coulon *et al.*,² is not in disagreement with experiment.

Theoretical results of comprehensive and *ab initio* calculations, as reported here, do not lend themselves to a thorough comparison with findings based on models as explained elsewhere.^{14,35} This situation is illustrated by the absence, in the standard Anderson Hamiltonian, of interactions between localized electrons as well as those between delocalized ones. These interactions are included in the Kohn-Sham Hamiltonian we employed. Only few previous calculations, comparable to ours, have addressed the issue of magnetism for 3d impurities in aluminum. Our results for the magnetic moments differ from those of Deutz *et al.*, except for chromium. We attribute the differences in part to their treatment of the aluminum potential which was assumed to be that of the elemental metal. A second source of difference consists of that of the systems; we considered free clusters, while they studied infinite systems. Optical measurements by Beaglehole and Wihl³⁶ showed that manganese impurities

drastically modify the band structure of the aluminum host. Such modifications are expected from most other $3d$ impurities. The excellent agreement between the $2.005\mu_B$ we found and the 2.00 value reported by Deutz *et al.*, in the case of chromium, is believed to result from the fact that both studies found the same value, 6.51 , for the total charge on the chromium impurity. For other systems where a significant electron transfer to or from the impurity was found, in our work and by experiment,³⁶ our results are different from those of Deutz *et al.*

We know of no experimental results, for the appropriate concentration of 5 at. % or for the free clusters studied here, to permit a meaningful comparison with our findings for V, Co, and Ni, except for the very early ones discussed above and that mostly entailed concentrations below 2 at. %. The local moments on Co, Fe, and Ni, respectively, $0.39\mu_B$, $0.14\mu_B$ or less, and $0.013\mu_B$, are small enough to be destroyed upon the immersion of the cluster in an infinite system. In this sense, these results indicate a possible nonmagnetic state for dilute alloys for these elements, as found by experiment. In the case of vanadium, a moment may still exist in films of concentrations 5 at. % or smaller, as the

larger local moment of $0.57\mu_B$ may not be totally quenched. This possibility is actually indicated by experiment, as noted in the above discussion of the analysis of susceptibility data by Cooper and Miljak.³¹

In summary, this work produced quantitative and qualitative properties of $3d$ impurities in aluminum which are mostly in agreement with available recent measurements for comparable geometry and concentrations. Our results further indicate the need for refined experimental studies, as performed by Hauser and co-workers,¹⁰ of the magnetic properties of these clusters and alloys.

ACKNOWLEDGMENTS

This work was supported in part by funding from the Louisiana Education Quality Support Fund (LEQSF), administered by the Louisiana Board of Regents, under Contract Nos. LEQSF (1986-89)A-RD-15 and LEQSF (95-98)-RD-A-23, and from the Department of the Navy, Office of Naval Research (ONR Grant No. N00014-93-1-1368), through the Timbuktu Academy.

*Deceased.

¹L. I. Kurkina, O. V. Farberovich, and V. A. Gorbunov, *J. Phys. Condens. Matter* **5**, 6029 (1993).

²V. de Coulon, F. A. Reuse, and S. N. Khanna, *Phys. Rev. B* **48**, 814 (1993).

³D. Guenzburger and D. E. Ellis, *Phys. Rev. Lett.* **67**, 3832 (1991); *Phys. Rev. B* **45**, 285 (1992).

⁴M. E. McHenry, D. D. Vvedensky, M. E. Eberhart, and R. C. O'Handley, *Phys. Rev. B* **37**, 10 887 (1991).

⁵Y. Jinlong, L. Huibin, and W. Kelin, *Phys. Rev. B* **44**, 10 508 (1991).

⁶P. P. Singh, *Phys. Rev. B* **43**, 3975 (1991).

⁷D. Shechtman, I. Blech, D. Gratias, and J. W. Cahn, *Phys. Rev. Lett.* **53**, 1951 (1984).

⁸R. A. Dunlap and K. Dini, *J. Phys. F* **16**, 11 (1986). Also see P. A. Banvel and P. A. Heiney, *Phys. Rev. B* **33**, 7917 (1986).

⁹T. G. Dietz, M. A. Duncan, D. E. Powers, and R. E. Smalley, *J. Chem. Phys.* **74**, 6511 (1981). See also V. E. Rondybe and J. H. English, *ibid.* **76**, 2165 (1982).

¹⁰J. J. Hauser, H. S. Chen, and J. W. Waszczak, *Phys. Rev. B* **33**, 3577 (1986).

¹¹D. Bagayoko, N. Brenner, D. Kanhere, and Callaway, *Phys. Rev. B* **36**, 9263 (1987).

¹²P. W. Anderson, *Phys. Rev.* **124**, 41 (1961).

¹³J. Kondo, in *Solid State Physics*, edited by F. Seitz, D. Turnbull, and H. Ehrenreich (Academic, New York, 1969), Vol. 23, pp. 183–281; A. J. Heeger, *ibid.*, pp. 283–411.

¹⁴D. K. Wohlleben and B. R. Coles, in *Magnetism*, edited by Harry Suhl (Academic, New York, 1973), Vol. 5, pp. 3–55.

¹⁵N. Andrei, K. Furuya, and J. H. Lowenstein, *Rev. Mod. Phys.* **55**, 331 (1983).

¹⁶R. M. Nieminen and M. Puska, *J. Phys. F* **10**, L123 (1980).

¹⁷J. Deutz, P. H. Dederichs, and Zeller, *J. Phys. F* **11**, 1781 (1981).

¹⁸A. V. Postnikov, V. I. Anisimov, and V. A. Gubanov, *Fiz. Met. Metalloved.* **54**, 251 (1982) [*Phys. Met. Metallogr. (USSR)* **54**(2), 36 (1982)].

¹⁹P. M. Boerigter, A. Lodder, and J. Molenaar, *Phys. Status Solidi B* **119**, K91 (1983).

²⁰E. Mrosan and G. Lehmann, *Phys. Status Solidi B* **87**, K21 (1978).

²¹G. Lautenschlager and Mrosan, *Phys. Status Solidi B* **91**, 109 (1979).

²²L. Dagens, *Phys. Status Solidi B* **93**, 279 (1979).

²³P. Blaha and J. Callaway, *Phys. Rev. B* **33**, 1706 (1986).

²⁴D. Bagayoko, P. Blaha, and J. Callaway, *Phys. Rev. B* **34**, 3572 (1986).

²⁵A. K. Rajagopal, S. P. Singhal, and J. Kimball (unpublished), as quoted by A. K. Rajagopal, in *Advances in Chemical Physics*, edited by G. I. Prigogine and S. A. Rice (Wiley, New York, 1979), Vol. 41, p. 59.

²⁶K. Lee, Ph.D. thesis, Louisiana State University, 1984, available from University Microfilms International Ann Arbor, Michigan 48106.

²⁷K. Lee, J. Callaway, and S. Dhar, *Phys. Rev. B* **30**, 1724 (1984).

²⁸J. W. Mintmire and B. W. Dunlap, *Phys. Rev. A* **25**, 88 (1983).

²⁹A. J. H. Watchers, *J. Chem. Phys.* **523**, 1033 (1970). For the Al basis set, see S. P. Singhal and J. Callaway, *Phys. Rev. B* **16**, 1744 (1977) or see Ref. 11.

³⁰C. Rizzuto, *Rep. Prog. Phys.* **37**, 147 (1974). For the interpretation of the low-field Hall coefficient measurements, please see C. Papastaikoudis and D. Papadimitropoulos, *Phys. Rev. B* **24**, 3108 (1981).

³¹J. R. Cooper and M. Miljak, *J. Phys. F* **6**, 2151 (1976). See also M. Miljak and J. R. Cooper, *Physica B* **86-88**, 476 (1977).

³²A. D. Caplin and C. Rizzuto, *Phys. Rev. Lett.* **21**, 746 (1968).

³³P. Steiner, H. Hochst, W. Steffen, and S. Hufner, *Z. Phys. B* **38**, 191 (1980). See also J. F. van Acker, Z. M. Stanik, J. C. Fuggle, H. J. W. M. Hoekstra, K. H. J. Buschow, and G. Stroink, *Phys. Rev. B* **37**, 6827 (1988).

³⁴R. A. Dunlap, D. J. Lloyd, I. A. Christie, G. Stroink, and Z. M. Stadnik, *J. Phys. F* **18**, 1329 (1988).

³⁵D. Riegel, L. Buermann, K. D. Gross, M. Luszik-Bhadra, and S. N. Mishra, *Phys. Rev. Lett.* **61**, 2129 (1988).

³⁶D. Beaglehole and M. Wihl, *J. Phys. F* **2**, 43 (1972).

³⁷K. Lee and J. Callaway, Phys. Rev. B **49**, 13 906 (1994).

³⁸K. J. Tauer and R. J. Weiss, Bull. Am. Phys. Soc. **6**, 125 (1961).

³⁹O. K. Anderson, J. Madsen, U. K. Poulsen, O. Jepsen, and J. Kollar, Physica B **86–88**, 249 (1976).

⁴⁰D. Bagayoko and J. Callaway, Phys. Rev. B **28**, 5419 (1983).

⁴¹V. Moruzzi, P. Marcus, and P. C. Pattnaik, Phys. Rev. B **37**, 8003 (1988). Also see V. Moruzzi, Phys. Rev. Lett. **57**, 2211 (1986).